

Miniaturized Dual-Polarized Ultra-Wideband Tapered Slot Antenna

Fuguo Zhu, Steven Gao Anthony TS Ho, Tim WC Brown Jianzhou Li, Gao Wei, Jiadong Xu
 University of Kent, Canterbury, UK University of Surrey, Guildford UK Northwestern Polytechnical University, Xi'an, China

Abstract—A compact dual-polarized tapered slot antenna is proposed for ultra-wideband (UWB) through-wall imaging applications. The dual-polarized antenna is obtained by shifting one single-polarized element orthogonally into the other one. The miniaturization of the antenna is realized by employing a folded balun comprising a folded slot on the right side of the radiator and a stepped microstrip line is used for improving the impedance matching. In addition, the fabrication complexity of the antenna is reduced due to the use of a folded balun. The antenna occupies a small size of $30 \times 30 \times 16 \text{ mm}^3$. Both simulated and measured results confirm that it can achieve a wide impedance bandwidth from 3.1 to over 12 GHz. Both ports have similar radiation characteristics with an isolation of 20 dB and the gain response is varying from 2.5 to 6.8 dBi.

Keywords: UWB antenna, dual-polarized antenna, tapered slot antenna, compact size, folded balun

I. INTRODUCTION

The allocation of the frequency range from 3.1 to 10.6 GHz has increasingly attracted much interest in various UWB applications including short-range, high-data-rate communication [1] and high-resolution imaging radar and sensor [2-3] due to its large bandwidth. The tapered slot antenna [4-5] is a promising candidate for UWB applications as it has many attractive characteristics: wide bandwidth, directional radiation patterns, low profile and easy fabrication.

Compared to single-polarized UWB antennas, the performance of imaging systems can be significantly improved by exploiting dual-polarized UWB antennas [6-7]. Moreover, the dual-polarized tapered slot antenna can be obtained by shifting two single-polarized elements orthogonally into each other [8]. In order to reduce the volume, a compact dual-polarized UWB tapered slot antenna of $35 \times 35 \times 53 \text{ mm}^3$ in [9] is realized by dielectric loading. It is also noticed that, the metallization on the backside of one element has to be interrupted to accommodate the other one, thus leads to increasing the fabrication complexity.

In this paper, a compact dual-polarized UWB tapered slot antenna with a folded balun is proposed. The size of the antenna is significantly reduced by employing the folded balun on one side of the element. In addition, the fabrication complexity of the prototype is eased due to the folded balun. To prove the concept, a prototype is developed and measured in the frequency domain. Both simulated and measured results are presented and discussed. The rest of the paper is organized as follows: the configuration and design of the single-polarized tapered slot antenna are demonstrated in Section II, Section III illustrates the design of the dual-polarized tapered

II. SINGLE-POLARIZED TAPERED SLOT ANTENNA

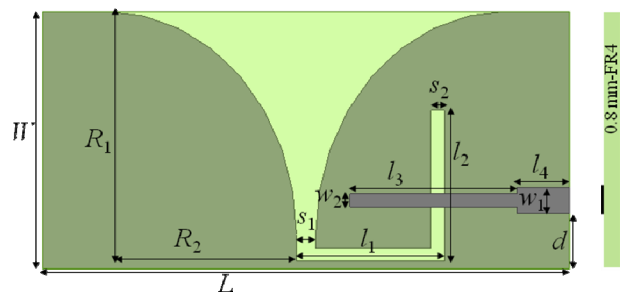


Figure 1. Geometry of the proposed single-polarized tapered slot antenna.

slot antenna. A conclusion is drawn in Section IV.

Figure 1 presents the geometry of the proposed single-polarized tapered slot antenna, which is printed on an FR4 substrate with a thickness of 0.8 mm and a relative permittivity of 4.55. The elliptical tapered slot is embedded in a rectangular plane on the bottom layer of the substrate and has major and minor radii of R_1 and R_2 respectively. The microstrip-line-to-slotline transition consists of a folded slot and a stepped microstrip line with distinct widths on the top layer of the substrate. The impedance matching of the antenna can be improved due to the stepped microstrip line. It is worthwhile to mention that, the right part of the radiator also behaves as a ground plane for the microstrip line. As the folded slot is inserted in the radiator and doesn't require additional space, the overall size of the antenna is miniaturized. Wideband performance can be achieved by selecting proper dimensions of the antennas. The optimized values of the dimensions are as follows: $W = 15 \text{ mm}$, $L = 30 \text{ mm}$, $R_1 = 14.55 \text{ mm}$, $R_2 = 12.1 \text{ mm}$, $l_1 = 8.4 \text{ mm}$, $l_2 = 8.8 \text{ mm}$, $l_3 = 9.5 \text{ mm}$, $l_4 = 3 \text{ mm}$, $s_1 = 1.1 \text{ mm}$, $s_2 = 0.75 \text{ mm}$, $w_1 = 1.52 \text{ mm}$ and $w_2 = 0.75 \text{ mm}$.

Since the microstrip-line-to-slotline plays an important role in the impedance matching of the antenna, four parameters l_1 , l_2 , l_3 , and l_4 are selected to study its effect. The parametric analysis is implemented while holding the remaining parameters with the optimized values. The effects on the reflection coefficient by the microstrip line and folded slot are illustrated in Figures 2 to 5. As shown in Figure 2, a wide frequency range for $|S_{11}| \leq -10 \text{ dB}$ is from 3.05 to over 12 GHz when the length of the horizontal slot l_1 is 8.4 mm. When it's too short, poor impedance matching near 4 and 11 GHz can be observed, while large l_1 leads to limited bandwidth. The result

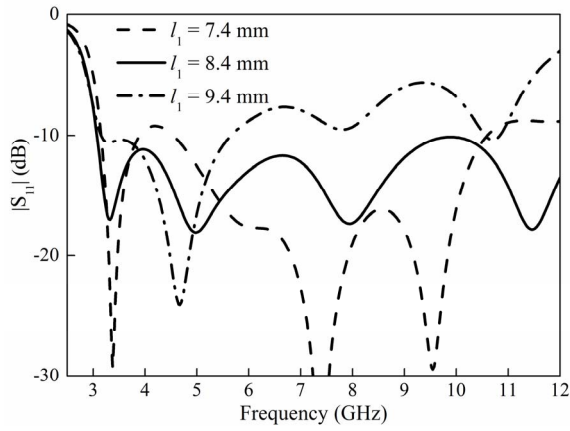


Figure 2. Effect of the horizontal slot l_1 on $|S_{11}|$.

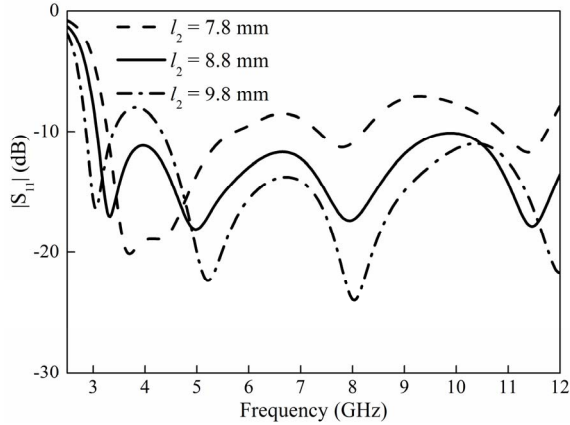


Figure 3. Effect of the vertical slot l_2 on $|S_{11}|$.

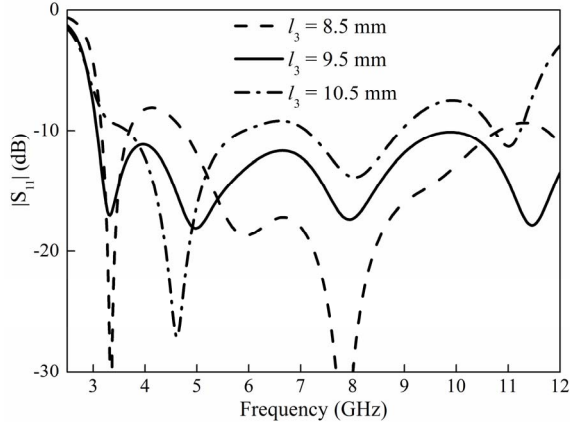


Figure 4. Effect of the narrow microstrip line l_3 on $|S_{11}|$.

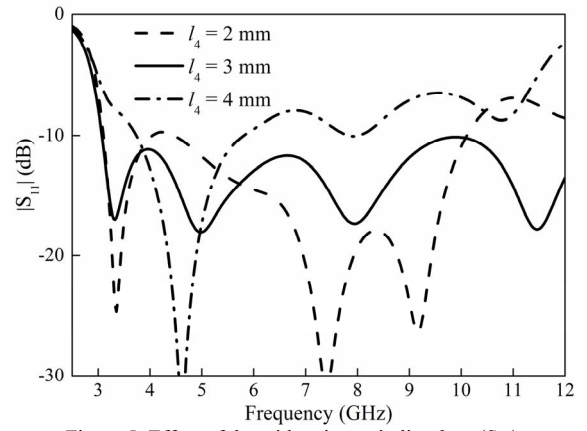


Figure 5. Effect of the wide microstrip line l_4 on $|S_{11}|$.

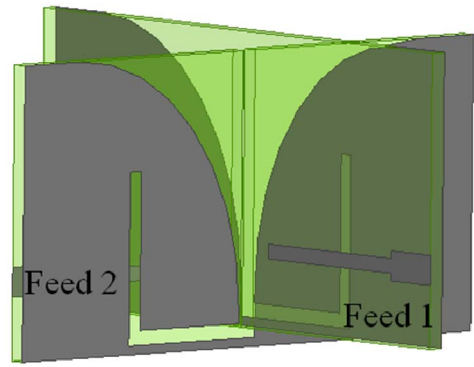


Figure 6. Geometry of the proposed dual-polarized tapered slot antenna.

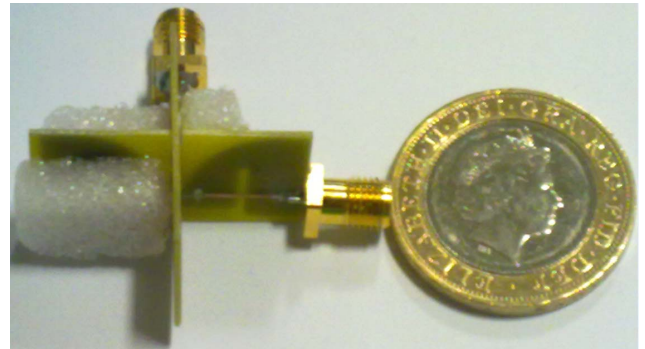


Figure 7. Photo of the fabricated prototype and a coin.

in Figure 3 indicates that short vertical slot causes poor impedance matching in the upper band whereas impedance mismatching in the lower band is observed when l_2 is larger than 8.8 mm. It is also noticed that the lowest operating frequency for $|S_{11}| \leq -10$ dB is ranging from 3.28 to 2.78 GHz when l_2 is increasing from 7.8 to 9.8 mm. The results in Figures 4-5 demonstrate that the effect of the microstrip line is similar to that of the horizontal slot. Limited bandwidth is obtained owing to the long microstrip line while short microstrip line will lead to poor impedance matching near 4 GHz. Interestingly, $|S_{11}|$ is larger than -10 dB near 11 GHz

when the length of the wide microstrip line is less than 3 mm. It can be summarized that, good impedance matching within a wide frequency band can be achieved by adjusting the dimensions of the microstrip-line-to-slotline.

III. DUAL-POLARIZED TAPERED SLOT ANTENNA

The configuration of the proposed dual-polarized tapered slot antenna is shown in Figure 6. The dual-polarized tapered slot antenna can be easily obtained by shifting one element (Antenna 1) orthogonally into the other one (Antenna 2). As observed, the metallization of Antenna 2 is not interrupted as Antenna 1 can be easily inserted into Antenna 2 by cutting a slot in the substrate of Antenna 2. The photos of the fabricated prototype and a coin are shown in Figure 7. The compactness of the antenna can be clearly observed when comparing it with

a coin. It is worth mentioning that the dimensions of the two elements are the same as the optimized parameters presented in Section II. The antenna doesn't need to be re-optimized. The dual-polarized tapered slot antenna has a volume of $30 \times 30 \times 16 \text{ mm}^3$. The position of Antenna 1 is shifted 1 mm with respect to Antenna 2. In order to verify the design concept, the prototype is measured and the results are compared with simulated results in the following part.

Simulated and measured results of reflection coefficient for two ports and mutual coupling between two ports are displayed in Figure 8. As observed, the simulated impedance bandwidths ($|S_{11}| \leq -10 \text{ dB}$) for port 1 and port 2 are 3.05-12 GHz, whereas corresponding measured results are 3.3-12 GHz and 3.2-12 GHz, respectively. A high isolation of 20 dB between two ports has been obtained over the whole operating frequency range.

The measured radiation patterns in two principal planes at different frequencies (3, 6, 9 and 12 GHz) for two ports are shown in Figures 9 and 10, respectively. The results in Figure 9 show that, the pattern in the E -plane is shifted off the end-fire direction at 3 GHz and omni-directional radiation in the H -plane can be observed at 3 GHz. At other frequencies, the patterns focus on the end-fire direction and have higher front-to-back ratio compared to 3 GHz. Figure 10 presents the measured radiation patterns for port 2. It is observed that the patterns for both ports have similar characteristics as they have the same dimensions.

Figure 11 presents the simulated and measured gain response for port 1 and port 2. As observed, the gain variations of the two ports have the same trend across the frequency band. The measured gain is found to be from 2.5 to 6.8 dBi.

IV. CONCLUSION

A compact dual-polarized tapered slot antenna with a size of $30 \times 30 \times 16 \text{ mm}^3$ has been presented in this paper. The volume of the antenna is significantly reduced owing to the use of the folded balun which consists of a folded slot and a stepped microstrip line. The antenna is excited by the microstrip line through a slot. In addition, it can help to ease the fabrication complexity of the prototype. The proposed antenna can achieve a wide frequency band from 3.1 to over 12 GHz with the antenna gain varying from 2.5 to 6.8 dBi for both ports. The measured mutual coupling between two ports is below -20 dB across the operating frequency range.

ACKNOWLEDGMENT

Authors wish to thank Prof. Raed A. Abd-Alhameed and Dr. Chan H. See at University of Bradford, UK for their help in the antenna measurement.

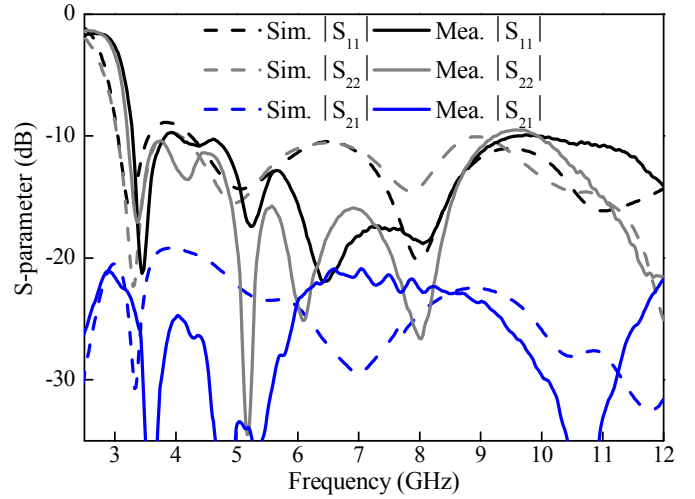


Figure 8. Simulated and measured results of S-parameters for the dual-polarized tapered slot antenna.

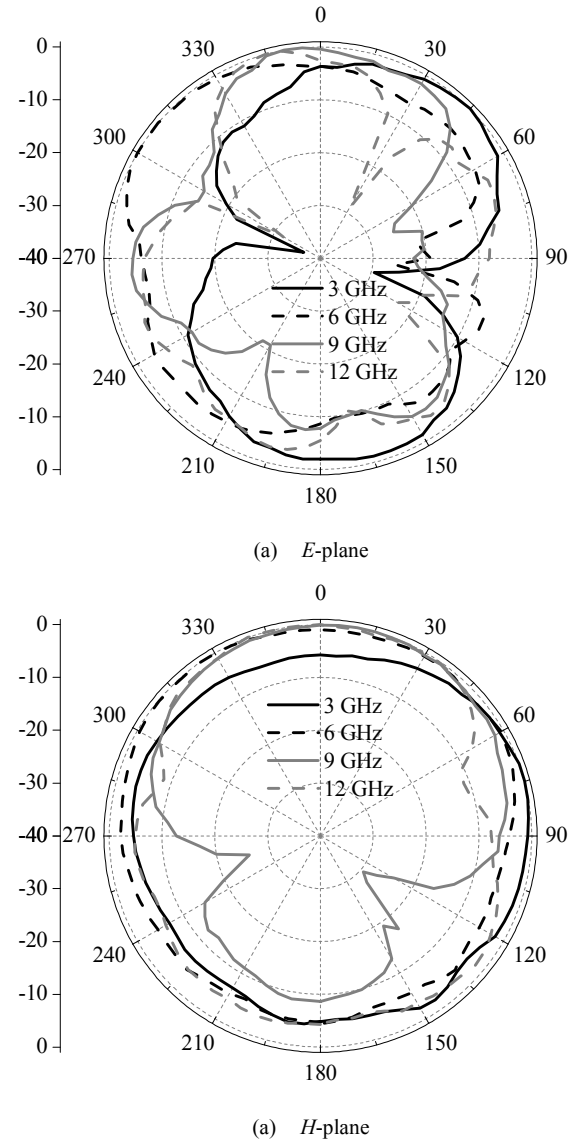
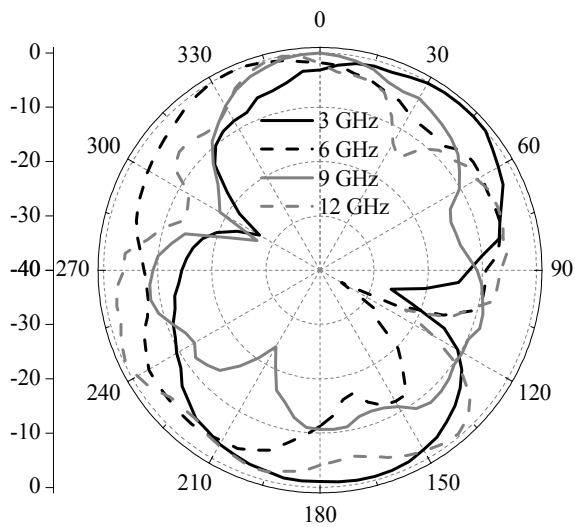
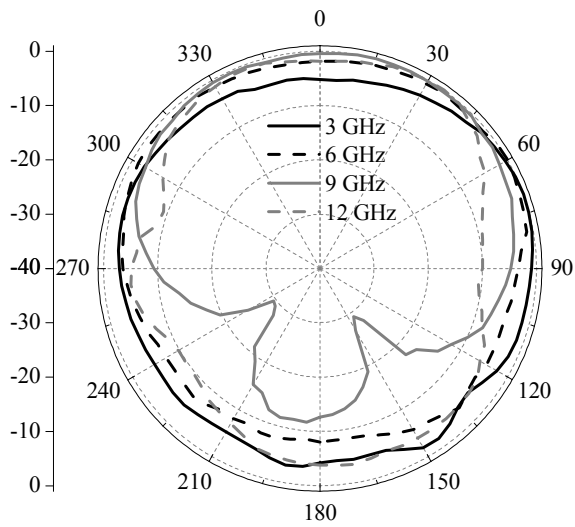


Figure 9. Measured radiation patterns at different frequencies for Port 1.



(a) *E*-plane



(a) *H*-plane

Figure 10. Measured radiation patterns at different frequencies for port 2.

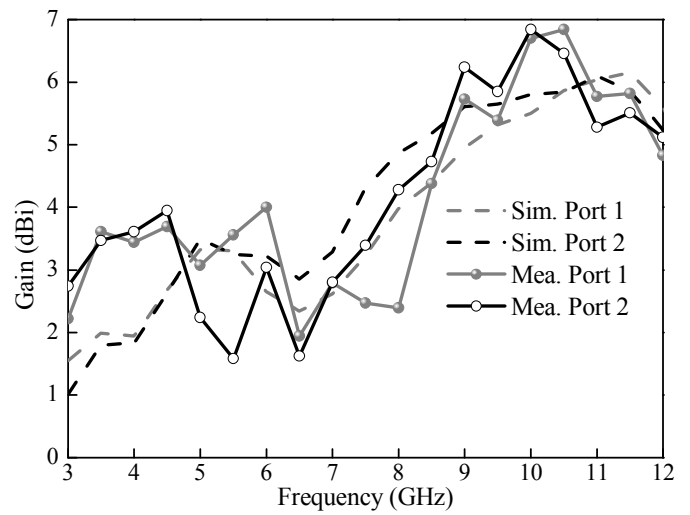


Figure 11. Simulated and measured gain response for port 1 and port 2.

REFERENCES

- [1] I. J. G. Zuazola, J. M. H. Elmighani, and J. C. Batchelor, "High-speed ultra-wide band in-car wireless channel measurements," *IET Commun.*, vol. 3, no. 7, pp. 1115-1123, 2009.
- [2] Y. Yang, and A. E. Fathy, "Development and implementation of a real-time see-through-wall radar system based on FPGA," *IEEE Trans. Geosci. Remote Sens.*, vol. 47, no. 5, pp. 1270-1280, 2009.
- [3] J. Li, Z. F. Zeng, J. Sun, and F. Liu, "Through-wall detection of human being's movement by UWB radar," *IEEE Geosci. Remote Sens. Lett.*, vol. 9, no. 6, pp. 1079-1083, 2012.
- [4] J. Shin, and D. H. Schaubert, "A parameter study of stripline-fed Vivaldi notch-antenna arrays," *IEEE Trans. Antennas Propagat.*, vol. 47, no. 5, pp. 879-886, 1999.
- [5] P. J. Gibson, "The Vivaldi aerial," *Proc. 9th European Microw. Conf.*, pp. 101-105, 1979.
- [6] X. Li, G. Adamiuk, M. Janson, and T. Zwick, "Polarization diversity in ultra-wideband imaging systems," *2010 IEEE International Conference on Ultra-Wideband (ICUWB)*, vol. 1, pp. 1-4, 2010.
- [7] L. Zwirello, G. Adamiuk, W. Wiesbeck, and T. Zwick, "Measurement verification of dual-orthogonal polarized UWB monopulse radar system," *2010 IEEE International Conference on Ultra-Wideband (ICUWB)*, vol. 2, pp. 1-4, 2010.
- [8] G. Adamiuk, T. Zwick, and W. Wiesbeck, "Dual-orthogonal polarized Vivaldi antenna for ultra-wideband applications," *17th International Conference on Microwaves, Radar and Wireless Communications*, pp. 1-4, 2008.
- [9] G. Adamiuk, T. Zwick, and W. Wiesbeck, "Compact, dual-polarized UWB- antenna, embedded in a dielectric," *IEEE Trans. Antennas Propagat.*, vol. 58, no. 2, pp. 279-286, 2010.